JSES International 4 (2020) 745–752

Contents lists available at ScienceDirect

JSES International

journal homepage: www.jsesinternational.org

Anatomic evaluation of radiographic landmarks for accurate straight antegrade intramedullary nail placement in the humerus

Peter S. Johnston, MD [a,*], Armodios M. Hatzidakis, MD [b], Yahia M. Tagouri, MD [c], Douglas Curran-Everett, PhD [d], Benjamin W. Sears, MD [b]

[a] Centers for Advanced Orthopaedics, Leonardtown, MD, USA
[b] Western Orthopaedics, Denver, CO, USA
[c] Medstar St. Marys Hospital, Leonardtown, MD, USA
[d] Division of Biostatistics and Bioinformatics, National Jewish Health, Denver, CO, USA

ARTICLE INFO

Keywords:
Proximal humerus fracture
intramedullary nail fixation
antegrade humeral nail
tuberosity fixation
straight intramedullary nail
fragility fracture

Level of Evidence: Anatomy Study; Cadaver Dissection

Background: Neurovascular insult, nonunion, and iatrogenic rotator cuff injury are concerns when using an intramedullary nail (IMN) for proximal humerus fracture. The purpose of this study was to identify a reproducible starting point and intraoperative imaging for nail insertion optimizing nail depth, tuberosity screw position, and protecting the axillary nerve and rotator cuff insertion. Our hypothesis was that a more medialized starting point would protect soft tissue structures and improve locking screw positioning.

Methods: Ten fresh-frozen cadavers underwent antegrade IMN with Grashey and modified lateral "precipice" view imaging. A guidewire was positioned medial to the coracoacromial ligament (CAL) in 5 cadavers and lateral to the CAL in 5. Distances from the nail entry point to anatomic landmarks were measured. Anatomic and histologic evaluations were performed, characterizing the nail perforation zone. Radiographs were compared between groups.

Results: The medial CAL group had a greater distance of screw fixation to the axillary nerve, a shorter distance of greater tuberosity (GT) screw fixation at the rotator cuff insertion on the infraspinatus and teres minor tubercles, and greater screw spread with improved lesser tuberosity capture. Two laterally placed implants violated the rotator cuff tendon. Imaging demonstrated that the ideal starting pin position was medial to the articular margin at a distance equal to the width of the rotator cuff insertion footprint.

Conclusions: Medial placement optimized fixation of the GT, avoided violation of the rotator cuff tendon and footprint, and was associated with an increased distance of proximal locking screw to the axillary nerve.

Fractures of the proximal humerus are the third most common fracture in patients older than 65 years, following hip and distal radius fractures,[17] with projected rates of emergency visits to exceed 275,000 annually by 2030.[9,17] Although most patients can be treated nonoperatively, displaced fractures and fractures with varus displacement can lead to poor patient-reported outcomes.[8,12] There are a number of described techniques for surgical treatment of displaced proximal humerus fractures, including percutaneous pinning, wire or suture fixation, locked plating, intramedullary nailing, locking cages, and joint replacement; however, no single technique has demonstrated evidence-based superiority over other implant options.[6]

Intramedullary fixation for proximal humerus fractures represents an alternative to open reduction and internal fixation with locked plating.[19] The reported benefits of intramedullary fixation include improved ability to preserve biology at the fracture site, the ability to fix segmental fractures with limited dissection, and the option for placement of the implant using a percutaneous technique with small incisions.[1] Further, the position of the nail in the proximal humerus provides an extra point of fixation in the humeral head that may help prevent varus collapse in fractures with medial comminution and calcar involvement. Alternatively, concerns about the use of nail fixation include iatrogenic rotator cuff injury during nail placement from either direct tendon injury during nail placement or with violation of the cuff footprint, risk for axillary nerve injury during proximal screw placement, and increased risk of nonunion due to inability to achieve direct bone-to-bone fixation and compression.[19]

Historically, intramedullary nails were designed with a proximal bend to avoid creating an articular cartilage defect in the proximal

No institutional review board approval was required for this study as no human research was conducted.

* Corresponding author: Peter S. Johnston, MD, 23000 Moakley Street, Suite 102, Leonardtown, MD 20650, USA.
E-mail address: Pjohnston4@hotmail.com (P.S. Johnston).

https://doi.org/10.1016/j.jseint.2020.06.004

humerus. However, this resulted in iatrogenic injury to the rotator cuff insertion as the starting point for these implants required device placement along the lateral articular margin either near or through the tendinous insertion. Violation of the rotator cuff insertion likely contributed to a reportedly high rate of unsatisfactory outcomes, with persistent pain being the predominant negative outcome predictor.[14] These poor results created the catalyst for the evolution in nail design changing the optimal position of implant insertion to a more medial position on the humeral head as to avoid violation of the rotator cuff footprint, resulting in report of improved outcomes in the literature.[7,19]

Despite a resurgence of interest in intramedullary fixation, little is known about optimal placement of the implant in the proximal humerus. Ideal positioning of the nail should optimize strength of the construct and minimize risk to surrounding soft tissue and neurologic structures. The ideal starting point for nail insertion following fracture reduction should minimize injury to the rotator cuff tendons and avoid violation of the cuff footprint on the tuberosity, avoid implant placement in fracture site, allow adequate nail depth in relation to the articular surface, and optimize screw tuberosity fixation to the nail and humeral head while minimizing the risk to the axillary nerve. The purpose of this study was to identify an ideal insertion point for placement of a straight intramedullary antegrade nail following fracture reduction with the goal of maximizing head and tuberosity fixation as well as protecting neurovascular structures. Further, we sought to identify reproducible radiographs for intraoperative nail placement to guide depth of insertion and screw placement. Our hypothesis was that a more medialized starting point for straight nail placement would protect surrounding soft tissue structures while improving positioning of the proximal locking screws.

Materials and methods

Ten fresh-frozen complete arm and scapula cadavers were allocated for this investigation. Specimens were thawed and prepared according to standard cadaveric preparation. The skin was removed in order to visualize the underlying shoulder anatomic structures. The entire origin of the deltoid was then carefully reflected from its attachment on the acromion and distal clavicle. The deltoid attachment on the humerus at the deltoid tuberosity was left intact, and the coracoacromial ligament (CAL) was carefully preserved and protected. The axillary nerve was identified and its course along the undersurface of the deltoid was marked with a marking pin. The distance of the axillary nerve from the midlateral acromion was measured and recorded. The specimen was then positioned on a Jackson spine table and placed in a surgical simulated fashion consistent with positioning of the operative extremity with the shoulder extended 20° posterior from midline, the scapula rotated 30° anterior from midline, and the arm in neutral rotation.

Two reproducible radiographs were obtained during nail placement for each specimen to monitor and document placement of guide pin, nail, and screws. A large C-arm was brought into the operative field from the contralateral side of the table. The standard anteroposterior (AP) radiograph was obtained with the C-arm beam perpendicular to the long axis of the humerus and arc orbit of approximately 30° toward the midline to obtain a Grashey view. This view was confirmed by identifying that the glenoid position was perpendicular to the beam of the imaging machine. This view also provided the most consistent profile view of the greater tuberosity (GT) with the arm in neutral rotation (Fig. 1, *a*).

The second radiograph was obtained by orbiting the machine over the top of the humerus to approximately 40°-45° of a lateral view. The beam was maintained at neutral or 10° caudad tilt from the perpendicular to the humerus, allowing for visualization of the profile of the posterior GT including the infraspinatus and teres minor tubercles. When positioned correctly, this view resembles a sloping mountain ridge, leading to coinage of the term *precipice* view (lateral view isolating the profile of the infraspinatous and teres minor tubercle on the GT; Fig. 1, *b*). From this view, determination of the accuracy of the guide pin placement from anterior to posterior was also assessed (Fig. 1, *c*).

Specimens were randomly selected and assigned to one of 2 groups, which would reproducibly result in a medial or lateral placement of the guide pin: (1) 5 specimens underwent nail placement with the guide pin placed either medial to or through the CAL (medial group) and (2) 5 specimens underwent nail placement with the guide pin placed lateral to the CAL (lateral group). The CAL was identified at its attachment on the acromion and left intact. For those specimens in the medial group, the guide pin was placed under direct visualization just anterior to the anterior acromion either through or medial to the CAL based on optimal positioning of the guide pin on imaging (Fig. 2). For the lateral cohort, the guide pin was placed lateral to the CAL, but in the most optimal position possible based on radiographs. In both groups, a sharp guide pin for the Tornier Aequalis (Wright Medical, Memphis, TN, USA) short intramedullary humeral nail was positioned using visual placement and radiographic confirmation with fluoroscopy. The guide pin was placed through the rotator cuff without any manipulation or formal splitting of the cuff tendon or muscle. When the guide pin was in acceptable position, standard Grashey AP and precipice lateral fluoroscopic images were obtained and saved. The starting cortical reamer was then placed over the guide pin and, with the reamer on full speed, manually pushed through soft tissue (CAL or rotator cuff muscle and/or tendon) to humeral cortical bone. A starting hole was made in the proximal humerus according to manufacturer specifications and the

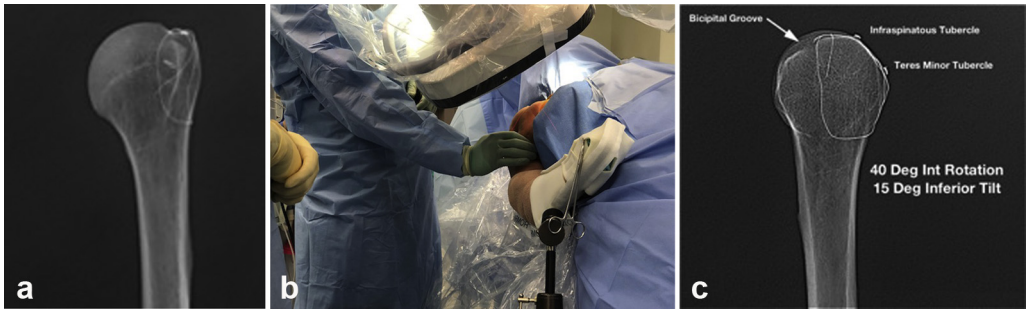

Figure 1 (**a**) Grashey radiograph of an isolated humerus with landmarks of the greater tuberosity isolated with steel wire. (**b**) Positioning of the C-arm to obtain the lateral "precipice view" image. (**c**) Lateral, or "precipice view," of the same isolated humerus demonstrating contour of greater tuberosity highlighting infraspinatus and teres minor tubercles. *Int*, internal.

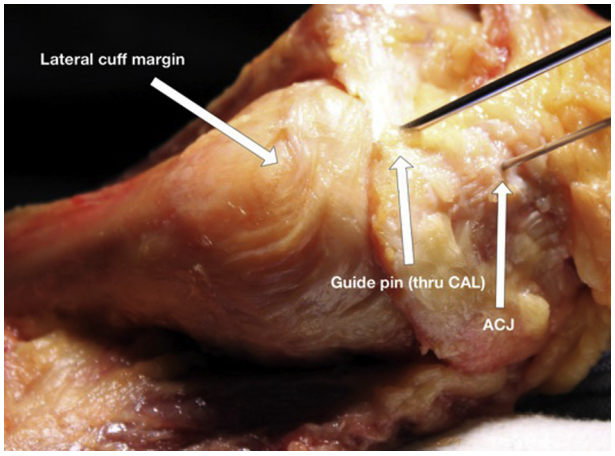

Figure 2 Starting pin position placed through the CAL. *CAL*, coracoacromial ligament; *ACJ*, acromioclavicular joint.

proximal metaphysis was reamed. The reamer was removed and the 8×130-mm intramedullary implant was then carefully placed into the intramedullary canal over the guidewire and under direct fluoroscopic evaluation. The deltoid origin was then anatomically repaired to the acromion with sutures.

The nail depth was obtained on all specimens using the precipice lateral view with the goal of placing the GT screws at the level of the infraspinatus tubercle (high screw) and teres minor tubercle (low screw) (Fig. 3). In addition, the implant guide arm was utilized, which has a radiographic marker that represents 5 mm from the marker to the proximal aspect of the nail and is useful to confirm the nail is completely seated underneath the subchondral bone. Nail rotation was based on the precipice lateral view ensuring the appropriate height and rotation for capture of the GT with high and low screws at the infraspinatus and teres minor tubercles, respectively. The epicondylar axis jig served as a secondary reference after radiographic verification. After nail depth was optimized, 4 interlocking screws were placed unicortically through the reduced deltoid using the guide arm and trocars per manufacturer recommendations.

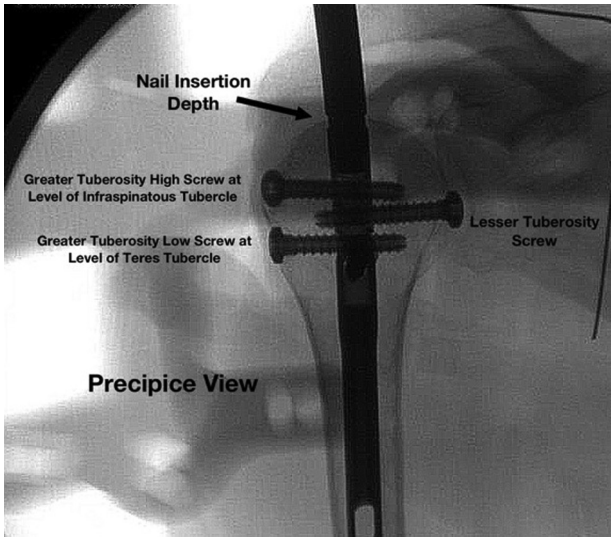

Figure 3 Precipice radiographic view following nail placement. The guide is still attached to the implant on this image.

The deltoid was then removed and proximity of the interlock screw trocar placement in relationship to the axillary nerve was measured and recorded. Screw heads were identified, and measurements in relation to important landmarks and implants were recorded (Fig. 4, *a* and *b*). The leading edge of the supraspinatus was marked with a suture, and the rotator cuff was reflected from its insertion on the GT and resected. The defect where the nail was placed was identified and visually inspected for the type of tissue violated by the nail (muscle, myotendinous, tendon). Measurements were made from the proximal humeral cortical defect to anatomic landmarks.

Final radiographs using standard fluoroscopic images were then obtained, including Grashey AP and precipice lateral views. All images were then transferred to a PACS imaging system for analysis. Radiographic measurements were made using a virtual "units" distance available on PACS. This was used because standard distance units of measure (eg, millimeters or centimeters) are not available with fluoroscopic imaging because of magnification inconsistencies. However, this also allowed for measurement standardization for each specimen by measuring consistent anatomic features and then applying those measurements as a ratio based on these standards. Anatomic features evaluated on Grashey AP imaging included the GT width (GTW) and distance from medial head to lateral tuberosity. The width of the humeral head from the anterior to the posterior cortical border was measured on the precipice lateral image. Radiographic measurements after the guide pin had been placed were made and quantified individually for each specimen based on previously obtained anatomic measurements. The distance of the medial border of the GT to guide pin, lateral aspect of the GT to the guide pin, and lateral humeral head articular surface to the guide pin were obtained from the Grashey AP images. The distance from the anterior head to guide pin as well as the distance from the posterior humeral head to the pin were obtained from the precipice lateral views.

Histologic analysis was also performed on the resected rotator cuff specimens to identify the specific region of rotator cuff tissue violated by the nail. The supraspinatus tendon from each cadaver was excised from the footprint to 1 cm medial to the nail penetration site. The muscle and tendon components were identified and labeled. The nail penetration site was identified and inked red. Specimens were submitted in 10% formalin for fixation for at least 2 weeks prior to processing for histopathologic evaluation by hematoxylin and eosin staining. Sections were taken at the point of nail penetration to identify exact points of entrance and exit. The slides were read by light microscopy and documented for the site of penetration and classified into 3 groups: muscular penetration only, tendon only, and penetration at the myotendinous junction.

Statistical analysis

We compared measurements between the 2 groups using 999,999 replications of a 2-sample permutation test.[2,4] RStudio (version 3.5.1, R Foundation for Statistical Computing, Vienna, Austria) was used to complete all data analyses.

Results

Anatomic analysis

Specimens were divided into 2 groups based on guide pin placement either lateral to, medial to, or through the CAL. The mean distance of the axillary nerve from the lateral acromion was identical between the groups: 61 mm for both the medial CAL and lateral CAL group ($P > .99$). The range for all 10 specimens in both groups was 50-80 mm.

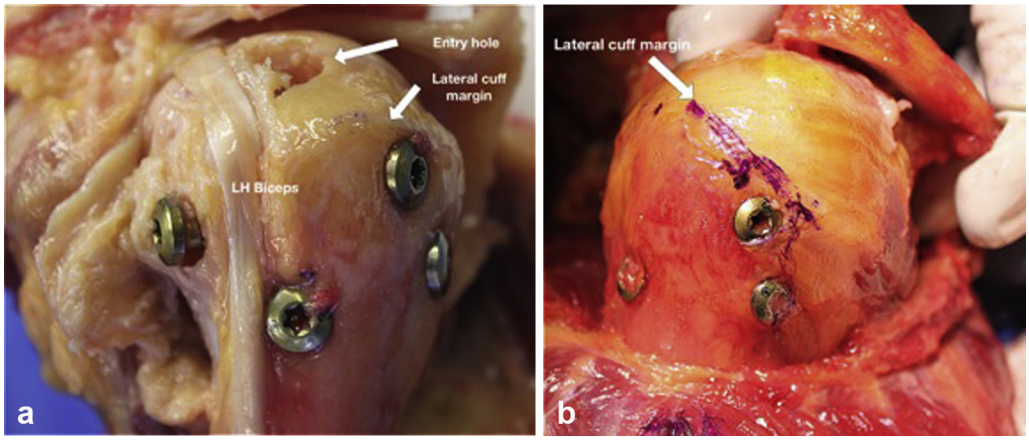

Figure 4 (**a**) Position of proximal humeral interlocking screws following placement of nail in relationship to the long head (LH) biceps tendon position. (**b**) Position of the greater tuberosity interlocking screws in relationship to lateral cuff margin.

For all specimens, the intramedullary implant was positioned in the most optimal position possible, dependent on guidewire position, based on radiographic analysis of nail insertional depth and tuberosity screw placement (based on proximity to the infraspinatus and teres tubercles). Comparison between these 2 groups demonstrated a number of significant differences regarding proximity of the intramedullary implant and peripheral screws to important anatomic structures between both groups (Table I). Position of the axillary nerve was farther from both GT screws in medial CAL specimens compared with lateral CAL specimens ($P = .08$ and $P = .07$); with 1 exception, position of the axillary nerve was also farther from the calcar screw in the medial specimens ($P = .07$). In addition, the lateral margin of the rotator cuff was significantly closer to the high GT and low GT screw in the medial CAL group compared with the lateral CAL group ($P = .04$ and $P = .05$), which correlates with an improved ability to place the screw on or near the higher-density bone at the infraspinatous and teres minor tubercle with the medial CAL group. Finally, maximal screw spread between the LT and low GT screws was significantly different between these groups, with the medial CAL group having an average screw spread of 58 mm and the lateral CAL group having an average screw spread of 41 mm ($P = .01$) (Fig. 5). Nail insertional depth was similar between the groups: 17 mm deep for medial CAL and 14 mm deep for lateral CAL ($P = .71$; see Fig. 3).

In terms of guide pin placement, there was difference between groups in the starting point lateral to the acromioclavicular joint (average medial CAL 1 mm [range 0-5 mm], lateral CAL 19 mm [5-35 mm], $P = .02$). There was also a difference in the proximity of the articular margin to the lateral aspect of the inserted nail (medial CAL 7 mm [4-10 mm], lateral CAL 1 mm [0-5 mm]; $P = .02$). Guide pin placement in relation to proximity of the bicipital groove and the long head of the biceps tendon was similar between the 2 groups (Fig. 4, *a*).

Table I
Specimen-specific measurements that resulted in a significant finding when comparing the 2 technique groups

Specimen no.	Starting point from AC joint	GTH (1) vs axillary nerve (mm)	GTL (3) vs axillary nerve (mm)	Calcar screw (4) vs axillary nerve (mm)	Articular margin to lateral edge of insertion (mm)	Maximal screw spread between LT and GTL (mm)	Acromion to axillary nerve (mm)	AP radiographic eval distance from medial GT to guide pin (mm)	AP radiographic eval distance from lateral GT to guide pin (mm)
Medial specimens									
7: Right 64F	4 mm lateral	40	35	20	8	64	65	54	92
2: Left 55F	0 mm	68	43	3	4	50	55	50	154
3: Left 62M	0 mm	40	24	18	10	58	60	84	155
4: Left 56F	2 mm medial	38	32	24	6	57	65	59	116
5: Right 77M	5 mm lateral	50	38	24	6	59	60	80	162
Lateral specimens									
1: Left 64F	8 mm lateral	22	14	5	0	29	60	39	116
6: Left 58F	20 mm lateral	21	9	10	2	48	62	17	60
8: Right 72F	5 mm lateral	42	36	7	0	45	80	11	54
9: Right 62F	35 mm lateral	40	26	15	0	35	54	-12*	38
10: Left 72F	25 mm lateral	25	20	4	5	47	50	23	77

AC, acromioclavicular; *GTH*, greater tuberosity high (screw); *GTL*, greater tuberosity low (screw); *LT*, lesser tuberosity; *GT*, greater tuberosity; *AP*, anteroposterior; *eval*, evaluation.
* Negative measure indicates measurement in the medial direction.

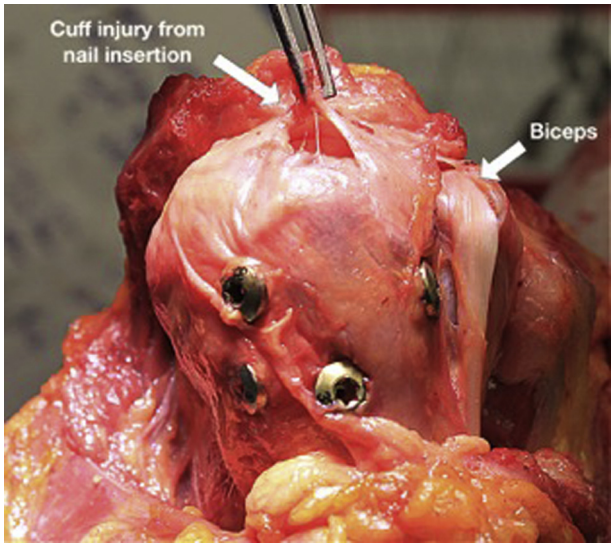

Figure 5 Violation of the cuff insertion following nail placement in a specimen in the lateral CAL cohort. Also notice narrow interlocking screw spread; the lesser tuberosity screw has been inserted lateral to the biciptal groove, missing the lesser tuberosity completely. *CAL*, coracoacromial ligament.

Radiographic analysis

Radiographic analysis was completed for each specimen after nail placement and anatomic evaluation. Each radiographic measurement was standardized by comparing measurements of guide pin placement relative to individual anatomic standards unique for each specimen. We then compared these ratios between both the medial CAL and lateral CAL groups. The groups were similar in terms of these anatomic features: GTW head width in the AP and medial and lateral planes. The distance from the guide pin to both the medial and lateral borders of the GT, expressed as a percentage of the GTW from Grashey AP imaging was greater in the medial CAL group than in the lateral CAL group ($P = .01$). In the medial CAL group, the guide pin was placed in the head medial to the medial aspect of the GT by an average distance equal to 103% of the GTW (range, 67%-135%) (Fig. 3); the guide pin was placed from the lateralmost aspect of the GT an average distance of 208% GTW (range, 166%-238%). In the lateral CAL group, the guide pin was placed in the head medial to the medial aspect of the GT by an average distance equal to 26% of the GTW (range −26% to +48%) (Fig. 6); the guide pin was placed from the lateralmost aspect of the GT an average distance of 128% GTW (range 83%-145%) in the lateral CAL group.

There were no additional significant guide pin measurement differences identified between the medial and lateral CAL groups. These measurements included the distance between the medialmost point of the humeral head articular surface to the guide pin and the position of the guide pin in the sagittal plane on the precipice lateral view, indicating that the overall positioning of the guide pin was consistent between the 2 groups. Anatomic and radiographic results are summarized in Table II.

Histologic evaluation

All rotator cuff entries occurred through the supraspinatus myotendinous unit. Violation occurred through the supraspinatus tendon in 2/10, myotendinous junction in 4/10, and through the muscle belly in 4/10. The medial CAL group was found to have 4/5 specimens with a starting point through muscle and 1/5 through the myotendinous junction. Of the lateral CAL group, 3/5 had a starting point through the myotendinous junction and 2/5 occurred through the rotator cuff tendon (Fig. 7). There were no footprint violations by the nail in any specimen.

Discussion

Interest in intramedullary treatment of displaced proximal humerus fractures has increased as a response to complication rates following locked plate fixation, a greater respect for fracture healing biology, and advances in nail design.[16,18] Initially, nails were designed with a proximal curvilinear bend to allow for insertion through a lateral entry point, thereby minimizing damage to the superior humeral articular cartilage. However, this design was found to have a higher incidence of postoperative pain secondary to rotator cuff footprint violation. Lopiz et al[14] demonstrated that 73% of bent nails led to symptoms related to rotator cuff pathology, as compared to 34.6% in the straight nail cohort. Also, the reoperation rate was reported at 42% in the bent nail group compared with 11.5% in the straight nail group. Nolan et al[15] also reported rotator cuff symptoms in more than than 50% of patients treated with bent humeral nailing, in addition to challenges with the lateral entry

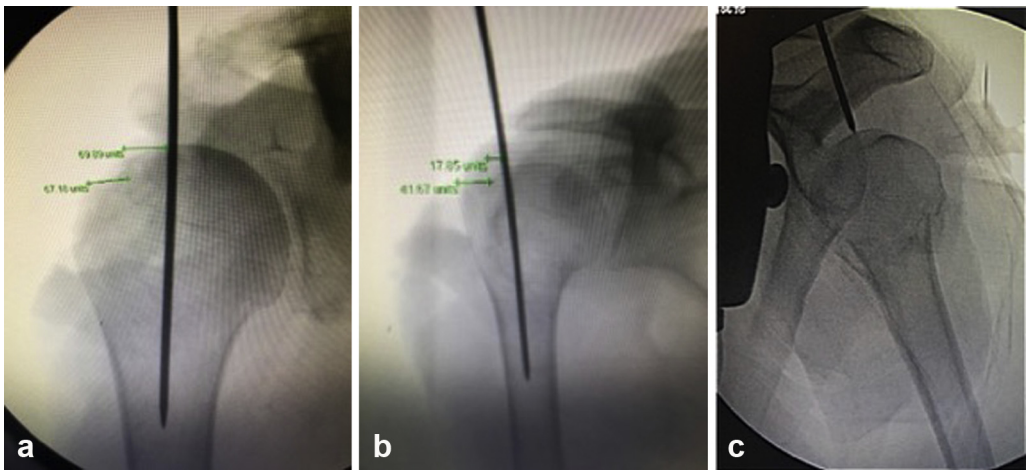

Figure 6 (**a**) Fluoroscopic Grashey view of the position of the guide pin in a medial CAL cohort specimen. The position of the guide pin is medial to the medial margin of the greater tuberosity by a distance equal to the greater tuberosity width (GTW). (**b**) Position of the guide pin in a lateral CAL cohort specimen (narrowed GTW). (**c**) Position of the guide pin on the precipice view. *CAL*, coracoacromial ligament.

Table II
Average measurement between landmarks

Measurement	Medial CAL group, mm, mean (range)	Lateral CAL group, mm, mean (range)	*P* value
GT high screw to axillary nerve	47 (38-68)	30 (21-42)	.08
GT low screw to axillary nerve	34 (24-43)	21 (9-36)	.07
Lateral margin of cuff to GT high screw	0.4 (−5 to 7)	6 (4-8)	.04
Lateral margin of cuff to GT low screw	0 (−5 to 4)	5 (0-20)	.05
Starting point from ACJ (lateral)	1 (4 lateral to 2 medial)	19 (8-35 lateral)	.02
Pin insertion in relation to CAL	1 (1 medial to 0)	5 (0-12 lateral)	.02
Max screw spread between LT and GT low screw	58 (50-64)	41 (29-48)	.01
Nail insertional depth	17 (12-28)	14 (8-20)	.71
Guide pin placement in relation to bicipital groove and LH biceps	5 (2-9)	8 (0-20)	.54
Articular margin to lateral aspect of insertion hole	7 (4-10)	1 (0-5)	.02
Calcar screw to axillary nerve	18 (3-24)	8 (4-15)	.07
Involvement of cuff tendon with insertion	• 4 through muscle • 1 through myotendinous junction	• 3 through myotendinous junction • 2 through tendon	n/a

GT, greater tuberosity; *ACJ*, acromioclavicular joint; *CAL*, coracoacromial ligament; *LT*, lesser tuborisity; *LH*, long head.
Distance of axillary nerve to lateral acromial (all specimens): average 61 mm (range, 50-80 mm)

point in proximity to the fracture site and reduced ability to obtain fixation in the humeral head.[5]

Straight nail designs allow for a more medialized starting point and centralized positioning within the humeral head, resulting in improved bone stock surrounding the implant and improving biomechanical stability of the bone-implant interface. Euler et al[3] coined this position as the fifth anchoring point and identified a "critical point" in a study of 200 computed tomographic (CT) scans of normal shoulders located at the most medial aspect of the supraspinatus footprint. Further, Lill et al[13] reported that the highest bone density was found in the most cranial aspects of the medial and dorsal regions of the proximal humerus correlating with the nail insertion point, whereas the lowest bone mineral density and the lowest mechanical rigidity were found in the central portion of the humeral head and at the GT where locked plate constructs typically achieve fixation. These findings suggest that the use of a humeral nail with optimal positioning and insertional depth can provide substantial biomechanical strength to the fixation construct that may be unavailable with other types of fixation.

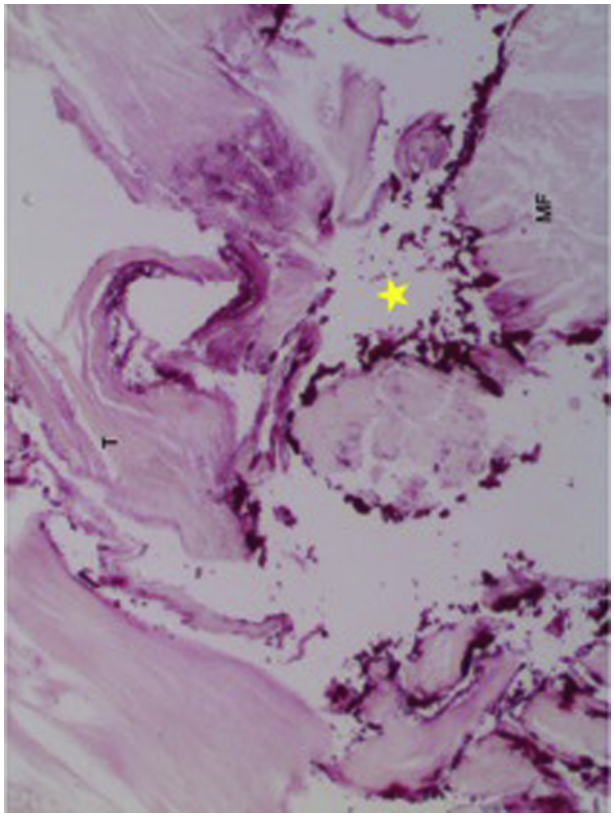

Figure 7 *Yellow star* indicates area of perforation at the rotator cuff myotendinous junction in a lateral CAL specimen. *CAL*, coracoacromial ligament.

Currently, there is a paucity of data in the literature regarding the ideal entry point for nail insertion and seating depth. In a cadaveric model, Euler et al[3] suggested using preoperative CT imaging of the contralateral extremity to help avoid iatrogenic injury to the rotator cuff. They identified 36% of humeri as "critical type," in which iatrogenic injury to the supraspinatus would occur given the 10-mm entry reaming required for available nails on the market. They concluded that CT of the contralateral side reliably identified the entry point and more importantly at-risk humeri for iatrogenic injury to the supraspinatus tendon. However, in the clinical setting, it is difficult to justify subjecting patients to the increased radiation dosage and cost of bilateral shoulder CT scans in order to identify these "critical type" humeri, particularly if nail placement could be preplanned and reproducibly implemented with the use of routine radiographic anatomic landmarks.

Additionally, there is a paucity of data with regard to soft tissue injury, particularly the intra- and extra-articular portions of the biceps tendon with intramedullary nailing. No reported series specifically identified biceps tendon iatrogenic injury as a result of nailing, but this is recognized as a potential complication, particularly with a percutaneous approach. Our data demonstrate that the intra-articular portion of the biceps tendon typically lies anterior to the nail insertion site at a mean distance of 6.6 mm (0-20 mm) from the anterior aspect of the reamed hole. Further, our data demonstrate that the bicipital groove falls a mean distance of 10.1 mm (3-21 mm) from the LT screw and a mean distance of 6.5 mm (0-20 mm) from the calcar screw.

In the current study, we identified the optimal starting point for placement of a humeral nail utilizing superficial anatomy and radiographic features, both of which may be used intraoperatively. We found that a medially placed humeral nail reduced the risk to surrounding soft tissue structures and improved implant fixation characteristics when compared to laterally placed implants, including proximity to the axillary nerve, tuberosity screw fixation points and screw spread, and rotator cuff tendon violation. In the cohort in which the IMN was placed medial to the CAL, high GT screw placement occurred at an average proximity of 47 mm from the

axillary nerve compared to 30 mm in the lateral group. This finding was similar for the low GT screws, which were significantly farther from the nerve in the medial CAL group at a distance of 34 mm as compared to the lateral CAL group at 21 mm. Calcar screws demonstrated the closest position to the axillary nerve in both groups (medial CAL average 18 mm, lateral CAL average 8 mm), although the difference between the groups did not reach significance. Based on these findings, it appears that a more medial starting point may help prevent iatrogenic injury to the axillary nerve.

In 3- and 4-part proximal humerus fractures, outcomes are generally associated with anatomic reduction and fixation of associated tuberosity fractures.[11] However, tuberosity fracture fixation can be tenuous given the relatively poor baseline bone quality at this area of the proximal humerus and potential for extensive comminution. Kirchhoff et al[10] investigated bone density of the GT in relation to anchor positioning during rotator cuff repair, finding that the posteromedial aspect of the GT has the highest bone density. This area corresponds to the infraspinatus and teres tubercle of the GT, which appears to be the ideal position of tuberosity fixation. Our data demonstrate that GT screw placement was significantly closer to the lateral cuff insertion and higher bone density of the tubercles in the medial CAL group compared to the lateral CAL group (average medial CAL 0.4 mm, average lateral CAL 6 mm). Furthermore, there was significantly increased screw spread between proximal humeral fixation points of the LT and GT screws in the medial CAL group (58 mm compared with 41 mm in the lateral CAL group), which correlates with distribution of the fixation strength over a broader area. It should be recognized that despite accurate radiographic localization, screw passage at the cuff insertion or through the tendon is possible.

Based on these anatomic findings, we found that a Grashey and modified lateral, or "precipice," radiographic image allowed for reproducible identification of anatomic landmarks that correlated with accurate nail placement. Radiographic data from this investigation demonstrate that placement of the guide pin on the Grashey view medial to the GT articular margin at a distance equal to the cuff footprint will maximize hardware distance from the axillary nerve, ensure placement of nail medial to cuff footprint, improve screw spread, and improve the ability to capture the lesser tuberosity with the corresponding screw. The "precipice" view provides the surgeon with an accurate identification of nail depth by verifying that the GT screws will capture the infraspinatus and teres tubercles where the best bone resides in the tuberosity (Fig. 1, *c*).

Conclusion

The current investigation demonstrates that a humeral nail placed in a more medial position results in increased distance of the hardware from the axillary nerve, rotator cuff tendon, and footprint and improves the fixation characteristics of the peripheral tuberosity screws. Clinically, this correlates to the placement of the nail guide pin immediately anterior to the acromion and approximately 1.5 mm lateral to the acromioclavicular joint at the location of the medial CAL acromial origin. Radiographically, the most optimal position of the guide pin is at the zenith of the humeral head, which correlates to approximately the width of the supraspinatus footprint medial to the articular margin, and equidistance anterior to posterior on the precipice view. The precipice view can also be used to confirm nail depth at a position that optimizes fixation of the peripheral screws at the infraspinatus and teres tubercles on the GT. Ultimately, routine intraoperative radiographs are sufficient to properly identify the medial starting point for a proximal humeral intramedullary nail.

Disclaimer

Wright Medical Technologies provided financial assistance for procuring cadaver specimens and donated the intramedullary nail (IMN) and screws used. Drs. Johnston, Sears and Hatzidakis receive research registry support for patients treated with the IMN utilized for this study.

Armodios M. Hatzidakis receives intellectual property royalties related for the intramedullary nail used in this study. He is a paid consultant for Wright Medical Technologies and receives research registry support for patients treated with the intramedullary nail used for this study.

Peter S. Johnston is a paid consultant for Wright Medical Technologies. He receives research registry support for patients treated with the intramedullary nail used for this study.

Benjamin W. Sears receives research registry support for patients treated with the intramedullary nail used for this study.

The other authors, their immediate families, and any research foundations with which they are affiliated have not received any financial payments or other benefits from any commercial entity related to the subject of this article.

Acknowledgments

The authors would like to acknowledge Libby Mauter, MS, PT, for her assistance in preparation of this manuscript.

References

1. Boileau P, d'Ollonne T, Bessière C, Wilson A, Clavert P, Hatzidakis AM, et al. Displaced humeral surgical neck fractures: classification and results of third-generation percutaneous intramedullary nailing. J Shoulder Elbow Surg 2019;28:276–87. https://doi.org/10.1016/j.jse.2018.07.010.
2. Curran-Everett D. Explorations in statistics: permutation methods. Adv Physiol Educ 2012;36:181–7. https://doi.org/10.1152/advan.00072.2012.
3. Euler SA, Hengg C, Kolp D, Wambacher M, Kralinger F. Lack of fifth anchoring point and violation of the insertion of the rotator cuff during antegrade humeral nailing: pitfalls in straight antegrade humeral nailing. Bone Joint J 2014;96-B:249–53. https://doi.org/10.1302/0301-620x.96b2.31293.
4. Good P. Confidence Intervals Based on Parametric Tests. In: Permutation, Parametric, and Bootstrap Tests of Hypotheses. 3rd ed. New York: Springer; 2005. p. 43–6.
5. Günther CM, Müller PE, Mutschler W, Sprecher CM, Milz S, Braunstein V. Straight proximal humeral nails are surrounded by more bone stock in comparison to bent nails in an experimental cadaveric study. Patient Saf Surg 2014;8:18. https://doi.org/10.1186/1754-9493-8-18.
6. Hasty EK, Jernigan EW 3rd, Soo A, Varkey DT, Kamath GV. Trends in surgical management and costs for operative treatment of proximal humerus fractures in the elderly. Orthopedics 2017;40:e641–7. https://doi.org/10.3928/01477447-20170411-03.
7. Hatzidakis AM, Shevlin MJ, Fenton DL, Curran-Everett D, Nowinski RJ, Fehringer EV. Angular-stable locked intramedullary nailing of two-part surgical neck fractures of the proximal part of the humerus. A multicenter retrospective observational study. J Bone Joint Surg Am 2011;93:2172–9. https://doi.org/10.2106/JBJS.J.00754.
8. Jung SW, Shim SB, Kim HM, Lee JH, Lim HS. Factors that influence reduction loss in proximal humerus fracture surgery. J Orthop Trauma 2015;29:276–82. https://doi.org/10.1097/BOT.0000000000000252.
9. Kim SH, Szabo RM, Marder RA. Epidemiology of humerus fractures in the United States: nationwide emergency department sample, 2008. Arthritis Care Res (Hoboken) 2012;64:407–14. https://doi.org/10.1002/acr.21563.
10. Kirchhoff C, Braunstein V, Milz S, Sprecher CM, Fischer F, Tami A, et al. Assessment of bone quality within the tuberosities of the osteoporotic humeral head: relevance for anchor positioning in rotator cuff repair. Am J Sports Med 2010;38:564-–9. https://doi.org/10.1177/0363546509354989.
11. Kloub M, Holub K, Polakova S. Nailing of three- and four-part fractures of the humeral head—long-term results. Injury 2014;45(Suppl 1):S29–37. https://doi.org/10.1016/j.injury.2013.10.038.
12. Krappinger D, Bizzotto N, Riedmann S, Kammerlander C, Hengg C, Kralinger FS. Predicting failure after surgical fixation of proximal humerus fractures. Injury 2011;42:1283–8. https://doi.org/10.1016/j.injury.2011.01.017.
13. Lill H, Hepp P, Korner J, Kassi JP, Verheyden AP, Josten C, et al. Proximal humeral fractures: how stiff should an implant be? A comparative mechanical study with new implants in human specimens. Arch Orthop Trauma Surg 2003;123:74–81. https://doi.org/10.1007/s00402-002-0465-9.

14. Lopiz Y, Garcia-Coiradas J, Garcia-Fernandez C, Marco F. Proximal humerus nailing: a randomized clinical trial between curvilinear and straight nails. J Shoulder Elbow Surg 2014;23:369–76. https://doi.org/10.1016/j.jse.2013.08.023.
15. Nolan BM, Kippe MA, Wiater JM, Nowinski GP. Surgical treatment of displaced proximal humerus fractures with a short intramedullary nail. J Shoulder Elbow Surg 2011;20:1241–7. https://doi.org/10.1016/j.jse.2010.12.010.
16. Owsley KC, Gorczyca JT. Fracture displacement and screw cutout after open reduction and locked plate fixation of proximal humeral fractures [corrected; erratum in: J Bone Joint Surg Am 2008;90:862]. J Bone Joint Surg Am 2008;90:233–40. https://doi.org/10.2106/jbjs.f.01351.
17. Palvanen M, Kannus P, Niemi S, Parkkari J. Update in the epidemiology of proximal humeral fractures. Clin Orthop Relat Res 2006;442:87–92. https://doi.org/10.1097/01.bio.0000194672.79634.78.
18. Thanasas C, Kontakis G, Angoules A, Limb D, Giannoudis P. Treatment of proximal humerus fractures with locking plates: a systematic review. J Shoulder Elbow Surg 2009;18:837–44. https://doi.org/10.1016/j.jse.2009.06.004.
19. Wong J, Newman JM, Gruson KI. Outcomes of intramedullary nailing for acute proximal humerus fractures: a systematic review. J Orthop Traumatol 2016;17:113–22. https://doi.org/10.1007/s10195-015-0384-5.